RESEARCH ARTICLE

Kaposi Sarcoma Herpesvirus Induces HO-1 during *De Novo* Infection of Endothelial Cells via Viral miRNA-Dependent and -Independent Mechanisms

Sara Botto,[a] Jennifer E. Totonchy,[b] Jean K. Gustin,[a] Ashlee V. Moses[a]

Vaccine and Gene Therapy Institute, Oregon Health and Science University, Beaverton, Oregon, USA[a]; Department of Pathology and Laboratory Medicine, Weill Cornell Medical College, New York, New York, USA[b]

ABSTRACT **Kaposi sarcoma (KS) herpesvirus (KSHV) infection of endothelial cells (EC) is associated with strong induction of *heme oxygenase-1* (HO-1), a stress-inducible host gene that encodes the rate-limiting enzyme responsible for heme catabolism. KS is an angioproliferative tumor characterized by the proliferation of KSHV-infected spindle cells, and HO-1 is highly expressed in such cells. HO-1 converts the pro-oxidant, proinflammatory heme molecule into metabolites with antioxidant, anti-inflammatory, and proliferative activities. Previously published work has shown that KSHV-infected EC *in vitro* proliferate in response to free heme in a HO-1-dependent manner, thus implicating virus-enhanced HO-1 activity in KS tumorigenesis. The present study investigated the molecular mechanisms underlying KSHV induction of HO-1 in lymphatic EC (LEC), which are the likely spindle cell precursors. In a time course analysis of KSHV-infected cells, HO-1 expression displays biphasic kinetics characterized by an early transient induction that is followed by a more sustained upregulation coincident with the establishment of viral latency. A viral microRNA miR-K12-11 deletion mutant of KSHV was found to be defective for induction of HO-1 during latency. A potential mechanism for this phenotype was provided by BACH1, a cellular *HO-1* transcriptional repressor targeted by miR-K12-11. In fact, in KSHV-infected LEC, the *BACH1* message level is reduced, BACH1 subcellular localization is altered, and miR-K12-11 mediates the inverse regulation of *HO-1* and *BACH1* during viral latency. Interestingly, the data indicate that neither miR-K12-11 nor *de novo* KSHV gene expression is required for the burst of HO-1 expression observed at early times postinfection, which suggests that additional virion components promote this phenotype.**

IMPORTANCE **While the mechanisms underlying KSHV induction of HO-1 remain unknown, the cellular mechanisms that regulate HO-1 expression have been extensively investigated in the context of basal and pathophysiological states. The detoxifying action of HO-1 is critical for the protection of cells exposed to high heme levels. KS spindle cells are erythrophagocytic and contain erythrocyte ghosts. Erythrocyte degeneration leads to the localized release of heme, creating oxidative stress that may be further exacerbated by environmental or other cofactors. Our previous work showed that KSHV-infected cells proliferate in response to heme and that this occurs in a HO-1-dependent manner. We therefore hypothesize that KSHV induction of HO-1 contributes to KS tumor development via heme metabolism and propose that HO-1 be evaluated as a therapeutic target for KS. Our present work, which aimed to understand the mechanisms whereby KSHV induces HO-1, will be important for the design and implementation of such a strategy.**

Received 21 April 2015 **Accepted** 29 April 2015 **Published** 4 June 2015

Citation Botto S, Totonchy JE, Gustin JK, Moses AV. 2015. Kaposi sarcoma herpesvirus induces HO-1 during *de novo* infection of endothelial cells via viral miRNA-dependent and -independent mechanisms. mBio 6(3):e00668-15. doi:10.1128/mBio.00668-15.

Invited Editor Dirk P. Dittmer, Center for AIDS Research (CfAR) **Editor** Herbert W. Virgin, Washington University School of Medicine

Address correspondence to Ashlee V. Moses, mosesa@ohsu.edu.

Kaposi sarcoma herpesvirus (KSHV, also known as human herpesvirus 8), an oncogenic gamma-2 herpesvirus, is the etiologic agent of the multifocal endothelial tumor known as Kaposi sarcoma (KS). KSHV infection can also result in primary effusion lymphoma (PEL), an aggressive non-Hodgkin B cell lymphoma, or multicentric Castleman disease, a systemic lymphoproliferative disorder (1–4). KSHV establishes persistent viral infection in endothelial and B cell targets by actively suppressing apoptosis and escaping immunodetection through various immune system evasion strategies (5, 6). These survival mechanisms are thought to contribute to host cell transformation and tumor development. We previously showed that *de novo* KSHV infection of human dermal microvascular endothelial cells (DMVEC) leads to upregulation of cellular heme oxygenase-1 (HO-1), a phenotype that is validated by the robust HO-1 expression observed in spindle cells in KS biopsy specimens (7, 8). Two functional HO isoforms, stress-inducible HO-1 and constitutive HO-2, have been identified. The HO-1 enzyme catabolizes heme into carbon monoxide, ferrous iron, and biliverdin. Regarding expression kinetics, HO-1 shows ubiquitous tissue distribution and is rapidly and strongly induced in response to various cellular stresses (9, 10). HO-1 is also highly expressed in several types of cancer. In the tumor setting, HO-1 is thought to contribute to cytoprotection, proliferation, and angiogenesis via the conversion of pro-oxidant, cyto-

toxic heme into metabolites with antioxidant, proangiogenic, antiapoptotic, and anti-inflammatory activities (10–15). Our previous work demonstrated that KSHV-infected DMVEC proliferate in response to low-dose heme and are protected from high-heme toxicity. We further showed that the proliferative and survival advantages of KSHV-infected EC were neutralized when HO-1 enzymatic activity was inhibited (7), suggesting an important role for the enzyme in KS pathophysiology. Despite an extensive body of literature describing the cellular regulation of HO-1 expression in both normal and pathological states (16–18), the mechanism(s) of HO-1 induction by KSHV remains to be defined.

MicroRNAs (miRNAs) are small noncoding RNA molecules that regulate gene expression post-transcriptionally. miRNAs are encoded by both animal and plant cells, as well as by the viruses that infect them (19, 20). Within the KSHV latency-associated region (KLAR) is encoded a set of viral proteins critical for the maintenance of the viral episome and for KSHV oncogenesis (21). Also encoded within the KLAR is a set of 12 miRNAs. Among these, miR-K12-11 is known to target the mRNA encoding the *HO-1* transcriptional repressor BACH1 (22, 23). BACH1 is a transcriptional repressor of genes such as *HO-1* that participate in the NRF2-dependent oxidative stress pathway (24). Under normal physiological conditions, NRF2 is prevented from entering the nucleus and activating transcription. However, under conditions of oxidative stress, NRF2 enters the nucleus and binds to the antioxidant response elements (AREs) found upstream of >200 antioxidant and cytoprotective genes (25), thereby activating their transcription. For a subset of these genes, BACH1 functions to counter NRF2 activation; under nonstress conditions, BACH1 binds to AREs, repressing the transcription of the associated genes. Interestingly, BACH1 is a heme-binding protein, which allows it to function as a heme sensor. Thus, above a toxic heme concentration, heme binds to BACH1 and causes BACH1 to disengage from the ARE, thereby alleviating HO-1 repression and allowing heme degradation (26, 27). BACH1 is then exported from the nucleus and degraded within the cytoplasm (28, 29). Targeting of the *BACH1* mRNA by miR-K12-11 thus enables KSHV to lower BACH1 levels, thereby deregulating oxidative stress pathways and facilitating infected-cell survival. Notably, miR-K12-11 exhibits high homology with cellular miR-155, which is also known to regulate *BACH1*. Cellular miR-155 is observed to be overexpressed in several types of B-cell lymphoma, and its ectopic expression in mice causes B-cell malignancies (30). Because cellular miR-155 and viral miR-K12-11 contain the same seed sequence (nucleotides 2 to 7 of the miRNA) required for their interaction with mRNAs, the two miRNAs have many targets in common, including *BACH1* (22, 23, 31, 32). Interestingly, miR-155 levels are not altered by KSHV infection, which suggests that miR-K12-11 functions in part by disrupting the regulation of host genes that are normally controlled by miR-155 (31). Several reports have described miR-K12-11 activity and function in both ectopic expression and non-endothelial *in vitro* infection systems (22, 23, 33). Additionally, miR-K12-11 has been shown to upregulate the expression of xCT, an amino acid transport protein subunit encoded by another ARE-containing gene, in EC, thereby protecting them from oxidative stress (34). However, the potential influence of miR-K12-11 on *HO-1* during *de novo* infection of EC has yet to be investigated.

In the present study, we explored the mechanisms whereby KSHV upregulates *HO-1* in lymphatic EC (LEC) at both early times postinfection and following the establishment of viral latency. We demonstrate that miR-K12-11 is one of the viral components responsible for *HO-1* upregulation during latency and that *HO-1* is transiently upregulated during the early phase of *de novo* infection via a mechanism that is independent of miR-K12-11 activity. We further show that miR-K12-11 targeting of the mRNA encoding the HO-1 transcriptional repressor BACH1 contributes to *HO-1* induction during latency.

RESULTS

KSHV infection modulates HO-1 expression in LEC in a biphasic manner. We previously reported the upregulation of *HO-1* expression in both primary and immortalized DMVEC latently infected with wild-type (WT) KSHV (7, 8). Using a recently developed KSHV bacterial artificial chromosome (BAC) system (KSHV-BAC16), we have confirmed the robust induction of HO-1 in LEC infected with BAC-derived recombinant KSHV (35). Considering both the recent recognition that LEC are the likely precursors of KS spindle cells and reports that KSHV induces lymphatic reprogramming of blood vascular EC (36–40), we decided to perform mechanistic studies with recombinant KSHV in lymphatic-lineage EC. We elected to use immortalized LEC (iLEC) for the majority of these studies because, like immortalized DMVEC, KSHV-infected iLEC can be maintained *in vitro* for the extended periods required for the establishment of viral latency (41). To initiate these mechanistic studies, iLEC were infected with BAC-derived WT KSHV (BAC16-WT) and cultured for 6 days to allow the establishment of latency. Cells were fixed, immunostained for both the viral latency protein LANA-1 (LANA) and HO-1, and then evaluated by deconvolution microscopy (Fig. 1A). Control cells expressed low basal levels of HO-1, with sporadic cells expressing slightly larger amounts. In contrast, infected cells, which were identified by LANA and green fluorescent protein (GFP) positivity, consistently expressed significantly higher levels of HO-1. In both mock-infected and virus-infected cells, HO-1 was localized predominantly to the cytoplasm, reflecting its well-characterized endoplasmic reticulum localization (42). Importantly, this pattern was also observed in mock-infected and KSHV-infected primary LEC (see Fig. S1A in the supplemental material). To determine the kinetics of HO-1 expression in infected iLEC, we performed a time course experiment measuring HO-1 mRNA (Fig. 1B) and protein (Fig. 1C) levels at sequential times postinfection. Using a reverse transcription-quantitative PCR (qPCR) assay, we observed induction of *HO-1* mRNA as early as 4 h postinfection (hpi). This early burst of expression was followed by a decline to basal levels by 24 hpi. Subsequently, coincident with the establishment of latency, HO-1 was reinduced, reaching a sustained phase of expression by 3 days postinfection (dpi) that persisted with time (Fig. 1B). HO-1 protein levels followed similar biphasic kinetics, with an early peak of expression at 6 to 8 hpi and sustained expression during latency (3 to 21 dpi). Parallel extended time course experiments with uninfected cells confirmed that long-term culture of iLEC had no impact on *HO-1* expression (see Fig. S1B). Thus, data from these experiments confirm that, similar to what we have previously described in both primary and transformed DMVEC (7), HO-1 is induced during KSHV latency. In addition, we now show that KSHV also alters HO-1 expression during the initial stages of *de novo* infection.

Our observation that the initial peak of HO-1 expression oc-

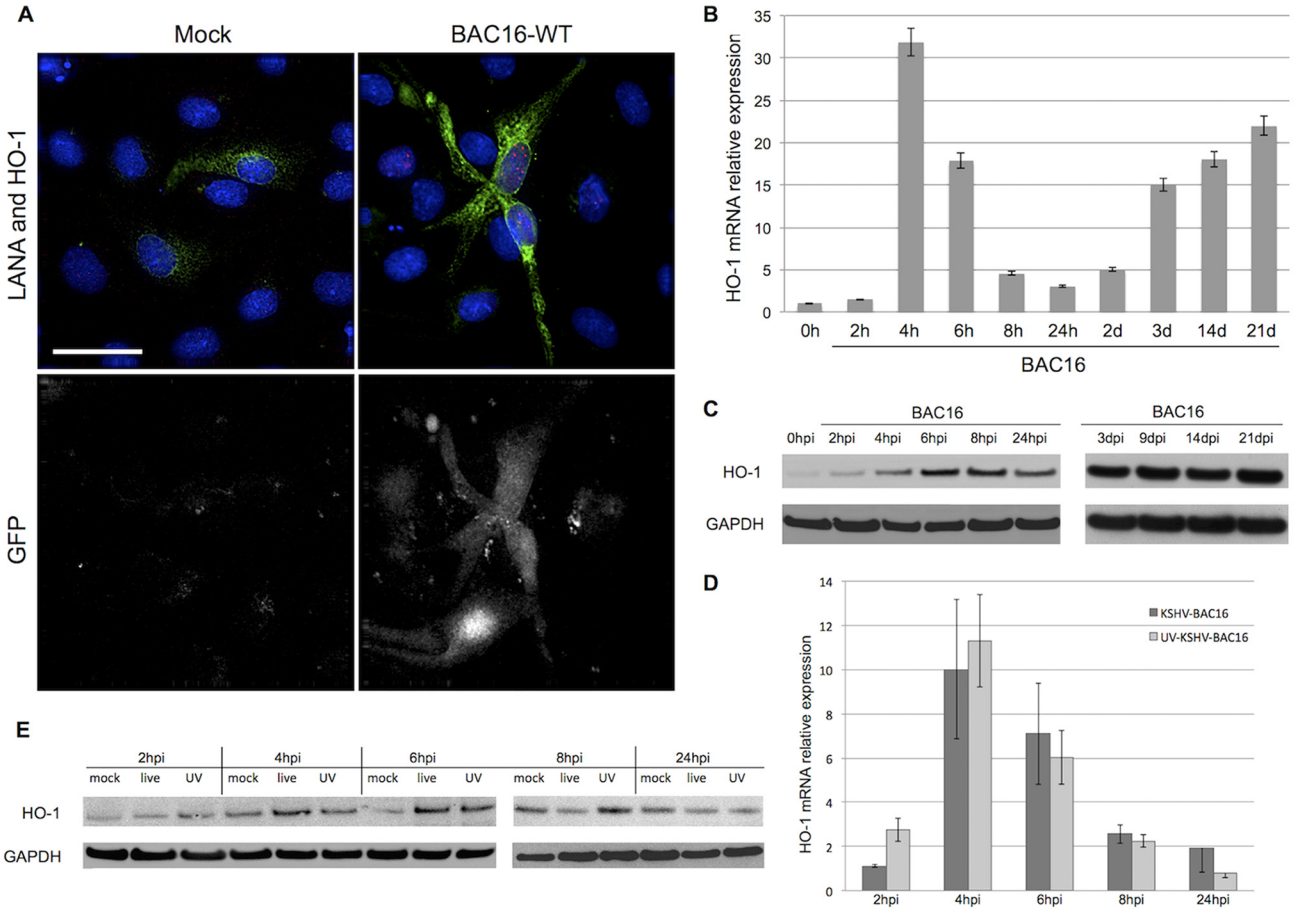

FIG 1 KSHV infection induces a biphasic induction of HO-1 in LEC. (A) IFA of mock-infected and KSHV-infected iLEC at 6 dpi. Top panels: LANA (red), HO-1 (green), and DAPI (blue). Bottom panels: GFP (grayscale, same cells as those shown in the top panels). The left panels correspond to mock-infected cells, and the right panels correspond to KSHV-infected cells. Images were captured at ×60 magnification (scale bar, 30 μm). (B) qPCR assay of mRNA levels for HO-1 in KSHV-infected iLEC at various times postinfection. Message levels are normalized to the GAPDH level, and fold change was calculated relative to mock-infected samples at each time point ($n = 3$). (C) WB assay showing HO-1 protein levels in KSHV-infected iLEC at various times postinfection. GAPDH was used as a loading control. (D) qPCR assay of *HO-1* mRNA levels in iLEC infected with either live or UV-inactivated KSHV. Cells were collected for analysis at the indicated times postinfection ($n = 3$). (E) A WB showing HO-1 protein levels in iLEC infected with either live or UV-inactivated KSHV. Cells were collected at the indicated times postinfection. GAPDH was used as a loading control.

curs within 4 h of virus exposure suggests that early HO-1 induction is independent of viral gene expression. Instead, HO-1 expression is likely to be triggered by a component(s) of the virus particle. To test this hypothesis, a time course experiment was performed in which iLEC were infected with either live or UV-inactivated BAC-derived KSHV. Samples were harvested at early times postinfection and then tested for both HO-1 mRNA (Fig. 1D) and protein (Fig. 1E) levels. The efficacy of UV inactivation was confirmed by our inability to detect both latent (LANA) and lytic (open reading frame 59 [ORF59]) viral transcripts from cells infected with UV-treated viral preparations (see Fig. S2A in the supplemental material). This finding was further corroborated by the lack of KSHV gene expression and the absence of HO-1 induction by UV-inactivated KSHV at later times postinfection (see Fig. S2B). Interestingly, at early times (0 to 24 h) postinfection, both live and UV-inactivated KSHV induced HO-1 to equivalent levels and with similar kinetics, indicating that *de novo* expression of viral genes is not required for the early peak of HO-1 expression. These experiments suggest that one or more components of the viral particle itself are responsible for the early transient expression of HO-1.

KSHV miR-K12-11 contributes to HO-1 induction during latent infection of LEC. It was recently reported that exogenous expression of KSHV-encoded miR-K12-11 was sufficient to induce HO-1 protein expression in 293 cells and that BACH1 levels were concomitantly reduced (43). In order to determine if miR-K12-11 influenced HO-1 levels in the context of *de novo* KSHV infection of LEC, we made use of a BAC16-derived KSHV mutant that no longer expressed functional miR-K12-11 (generously provided by Rolf Renne, University of Florida, Gainesville, FL). This mutant was generated by deleting one arm of the pre-miRNA, which prevents maturation to the active miRNA (44). For these experiments, iLEC were infected with the WT or a mutant virus lacking either miRNA-K12-11 or miRNA-K12-1 (included as a control mutant virus; also provided by Rolf Renne) and then cultured for 6 days to allow the establishment of stable latency. Proper expression of miR-K12-11 in WT virus-infected cells was confirmed by stem-loop qPCR assay (see Table S1 in the supple-

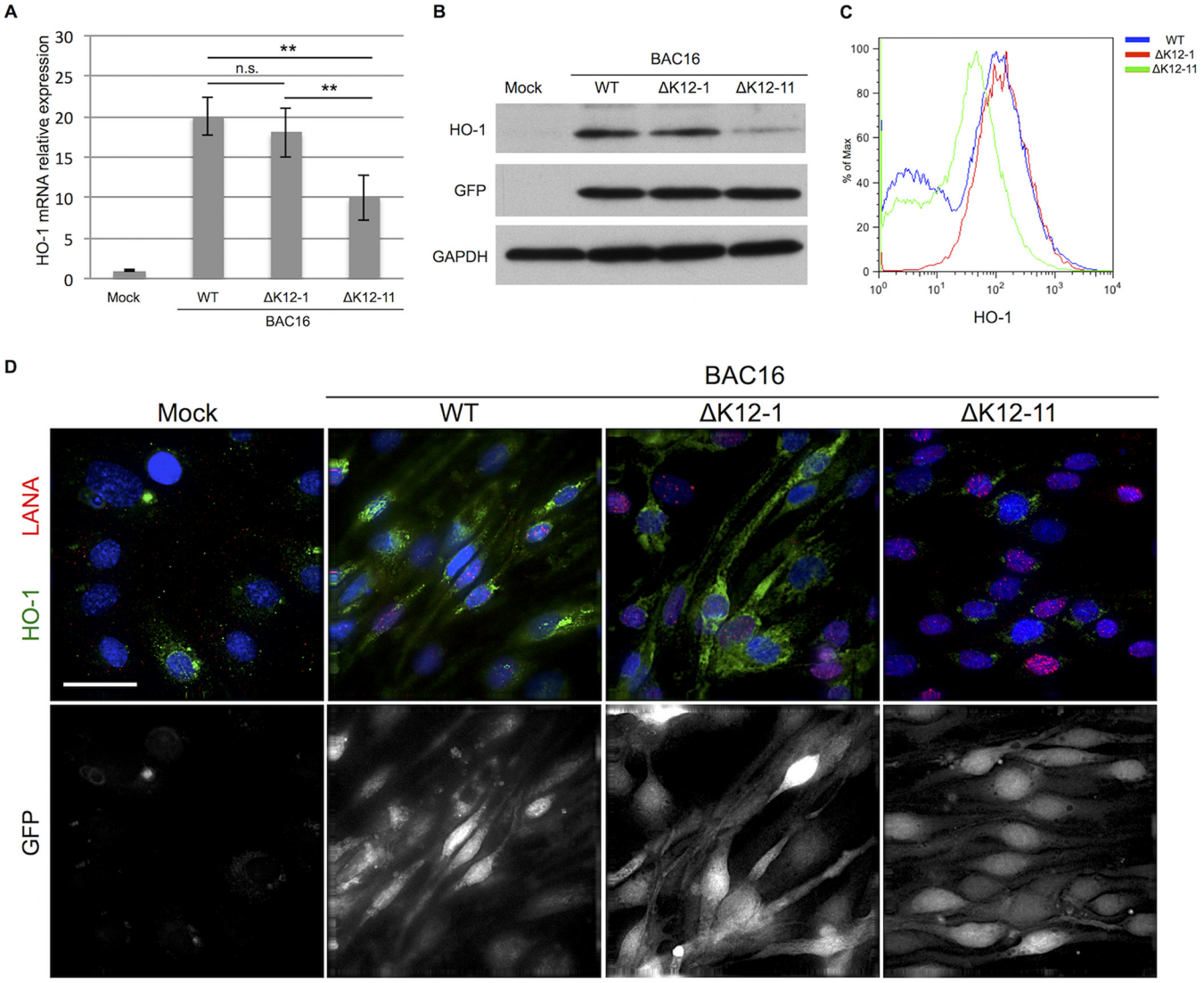

FIG 2 The KSHV ΔK12-11 mutant induces reduced levels of HO-1 in latently infected LEC. Time course experiments show HO-1 protein and mRNA levels at 6 dpi in iLEC infected with WT or ΔK12-11 or ΔK12-1 mutant (as a control) KSHV ($n = 3$). (A) qPCR assay results. n.s., not significant, **, $P \leq 0.01$. A one-way ANOVA was used for statistical analysis. (B) WB analysis. GAPDH was used as a loading control. (C) Flow cytometric analysis of infected cells gated on GFP. (D) IFA images. Top panels: HO-1 (green), LANA (red), and DAPI (blue). Bottom panels: GFP in grayscale (same cells as those shown in top panels). Images were captured at ×60 magnification (scale bar, 30 μm).

mental material). Compared to iLEC infected with either the WT or the control mutant (ΔK12-1), we observed significantly lower levels of HO-1 mRNA and protein (Fig. 2A and B) in iLEC infected with the ΔK12-11 mutant. Although HO-1 expression in ΔK12-11 mutant-infected cells was substantially reduced, some induction above basal levels in mock-infected cells was observed, indicating that KSHV induction of HO-1 during latency is not regulated exclusively by miR-K12-11. Flow cytometric analysis (Fig. 2C) of KSHV-infected (GFP-positive) iLEC confirmed the reduced HO-1 levels in cells infected with the ΔK12-11 mutant. Similarly, an indirect immunofluorescence assay (IFA) (Fig. 2D) demonstrated a clear decrease in cytoplasmic HO-1 expression in ΔK12-11 mutant-infected cells. In summary, these experiments support a key role for miR-K12-11 in HO-1 induction during latent KSHV infection of LEC. At the same time, our data show that additional viral and/or cellular factors contribute to maximal HO-1 expression in latently infected cells. Since miR-K12-11 is a viral ortholog of miR-155, we also considered the possibility that KSHV infection could influence the expression of miR-155 in LEC. In keeping with a previously published study with B cells, however (31), the expression of miR-155 in LEC was unaffected by KSHV infection (see Fig. S3 in the supplemental material).

Exogenous miR-K12-11 restores HO-1 expression in KSHV ΔK12-11 mutant-infected LEC. To provide further support for the hypothesis that miR-K12-11 plays a role in HO-1 induction during latent KSHV infection of LEC, a miR-K12-11 mimic was tested for the ability to complement the HO-1 induction defect observed for the ΔK12-11 mutant virus. This was accomplished by infecting iLEC with either WT or ΔK12-11 virus for 6 days, transfecting the cells with 100 ng of either a negative-control miRNA or a miR-K12-11 mimic, and then testing for levels of both HO-1 and miR-K12-11 at 24 hpi. Confirming the results shown in Fig. 2, in

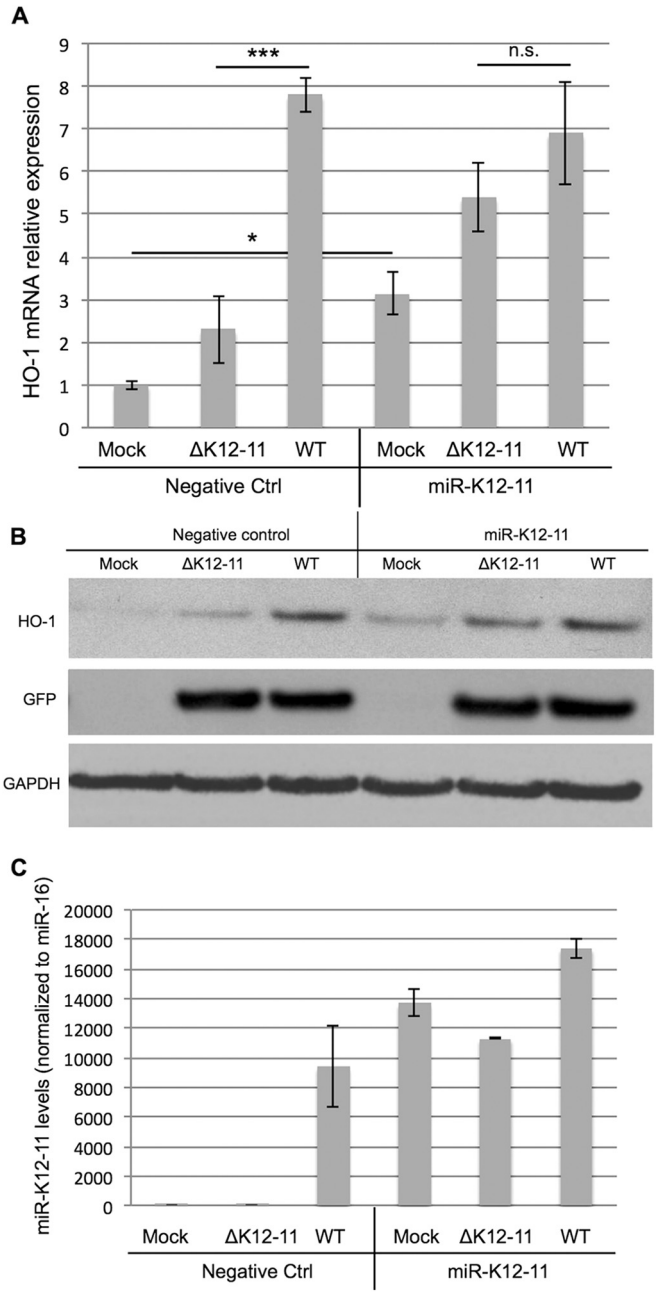

FIG 3 Exogenous expression of miR-K12-11 partially restores HO-1 induction in ΔK12-11 mutant-infected LEC. iLEC were sequentially infected with WT or ΔK12-11 mutant KSHV for 6 days, transfected with a miR-K12-11 mimic, and then incubated for another 24 h. Samples were then harvested and prepared for various HO-1 assays. (A) qPCR analysis. For each sample, the data were normalized to the GAPDH level and the fold change was determined relative to the mock-infected sample ($n = 3$). n.s., not significant; ***, $P \leq 0.0001$; *, $P \leq 0.05$. A one-way ANOVA was used for statistical analysis. (B) WB assay showing HO-1 protein levels. GAPDH was used as a loading control. (C) Demonstration of miR-K12-11 levels as determined by stem-loop qPCR assay. miR-K12-11 levels are normalized to the expression of the internal control miR-16 ($n = 3$).

cells infected with the ΔK12-11 mutant and then transfected with the control miRNA, HO-1 message (Fig. 3A) and protein (Fig. 3B) levels were 3- to 4-fold lower than those in similarly transfected cells infected with the WT virus. Conversely, in the presence of the miR-K12-11 mimic, HO-1 levels in ΔK12-11 mutant-infected cells were restored to levels approaching those seen in cells infected with the WT virus. Transfection of mock-infected cells with the miR-K12-11 mimic was sufficient to induce the HO-1 message and protein (Fig. 3A and B), which demonstrates that the KSHV miRNA alone is able to induce HO-1 expression. Stem-loop qPCR assay results (Fig. 3C) confirmed that the expression levels of miR-K12-11 in transfected cells were comparable to those in cells infected with the WT virus.

The HO-1 transcriptional repressor BACH1 is downregulated and redistributed in KSHV-infected LEC. As discussed above, the function of BACH1 is influenced by both its abundance and its subcellular localization. It has been previously shown that BACH1 protein levels are low in the stably KSHV-infected PEL cell line BCBL-1 and that miR-K12-11 plays a role in this phenotype (45). However, since BACH1 levels have not been examined in the context of a *de novo* KSHV infection in EC, we investigated BACH1 expression in LEC at 6 dpi with either WT or ΔK12-11 mutant virus. While WT-infected iLEC expressed significantly less BACH1 mRNA (Fig. 4A) and protein (Fig. 4B) than mock-infected cells did, BACH1 levels were not significantly reduced in cells infected with the ΔK12-11 mutant. Interestingly, IFA revealed that in KSHV-infected cells, BACH1 was consistently redistributed to the cytoplasm and that this redistribution occurred even in the absence of miR-K12-11 (Fig. 4C). Thus, our data indicate that *de novo* KSHV infection of LEC results in a decrease in the total BACH1 protein, dependent on miR-K12-11, and in its redistribution to the cytoplasm, which appears to be miR-K12-11 independent. The identities of the other viral and/or cellular components that are responsible for BACH1 relocalization are under investigation.

To further examine the contribution that BACH1 makes to the downregulation of HO-1 in the context of KSHV infection, we next asked if ectopic BACH1 expression could overcome KSHV-induced HO-1 induction in infected iLEC. For these studies, we expressed BACH1 from the adenoviral vector pAdTET7 (46). Expression of BACH1 from the adenoviral vector AdBACH1 was verified by IFA of transduced iLEC (see Fig. S4 in the supplemental material). In subsequent studies, latently infected iLEC were transduced with AdBACH1 or with the transactivator only (trans, as a control), and then HO-1 levels were examined 1 day later. In cells not infected with KSHV, adenoviral expression of BACH1 reduced basal HO-1 protein levels below the limit of detection (Fig. 4E), while mRNA levels could not be further reduced below the existing detection threshold (Fig. 4D). In KSHV-infected cells, the high levels of HO-1 message and protein that we typically observe were significantly reduced by BACH1 overexpression. Thus, our data show that ectopic expression of BACH1 can effectively overcome KSHV-dependent HO-1 induction.

KSHV induces HO-1 in LEC at early times postinfection in a miRNA-independent manner. Figure 1 shows that that as early as 4 hpi, KSHV transiently induces HO-1 and that this induction does not depend upon *de novo* viral gene expression. A previous study has shown that KSHV miRNAs, including miR-K12-11, can be detected in viral particles and that these miRNAs remain active even after UV inactivation (47). In light of this finding, we asked if miR-K12-11 could be delivered to host cells within the virus particle, thereby inducing the early peak of HO-1 expression. We first examined purified virus preparations for their miRNA content, and we found that a standard, purified WT virus preparation

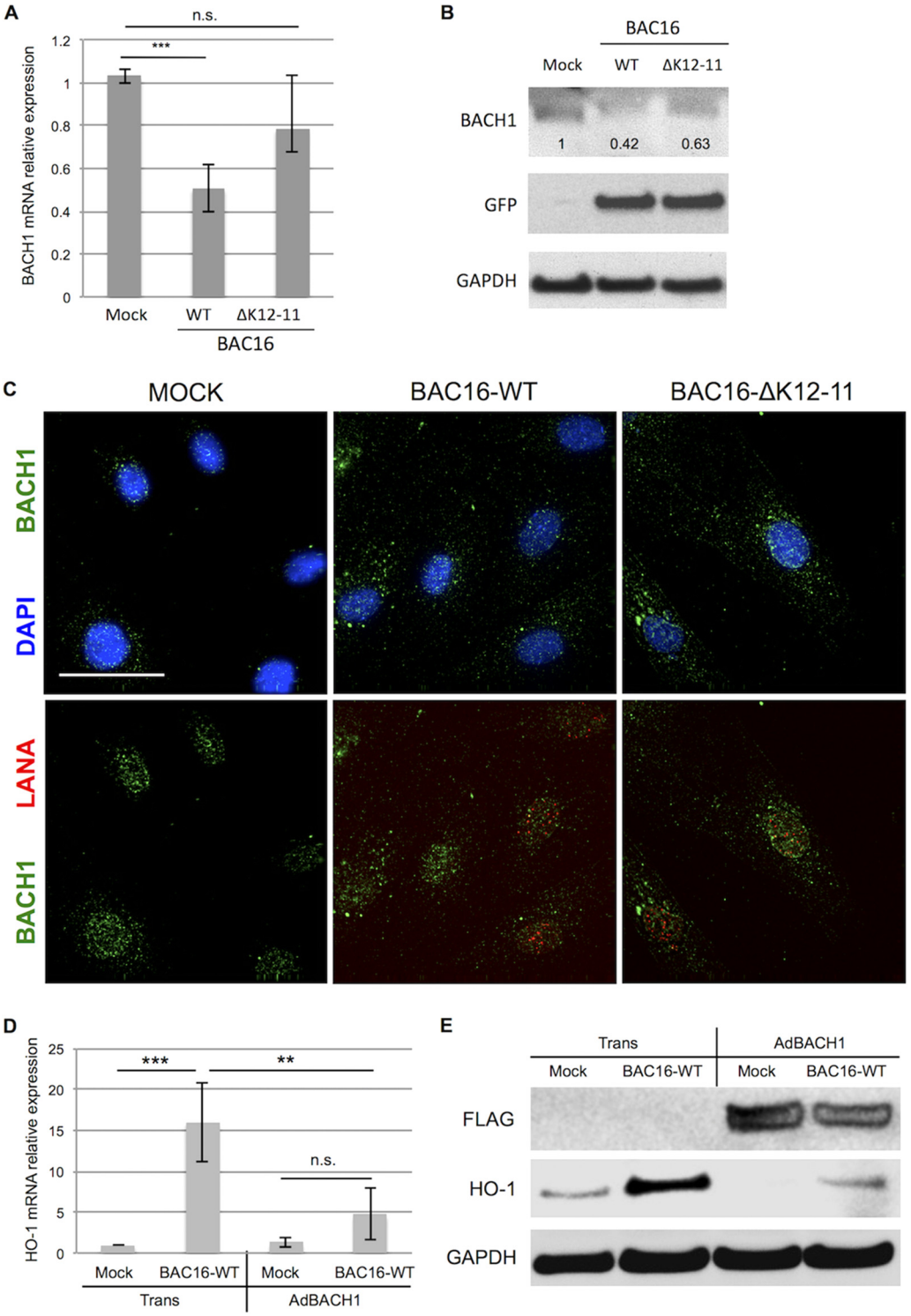

FIG 4 BACH1 levels and subcellular location are altered in KSHV-infected LEC. (A to C) iLEC were mock infected or infected with either the WT or ΔK12-11 mutant virus, samples were harvested at 6 dpi, and then BACH1 levels were determined. (A) qPCR analysis. The raw data for each sample were first normalized to those for GAPDH. The normalized data were then compared to those for the mock-infected sample in order to determine the fold change ($n = 6$). n.s., not significant; *, $P \leq 0.05$. Significance was determined with a Kruskal-Wallis test. (B) BACH1 WB assay. GFP expressed by the virus was used as marker of infection; GAPDH was used as a loading control. (C) IFA images. Top row, DAPI (blue) and BACH1 (green); bottom row, BACH1 (green) and LANA (red). Labels at the top of each panel correspond to the viruses used. Images were recorded at ×60 magnification; scale bar, 30 μm. (D and E) iLEC were first infected with the WT virus for 6 days and then transduced with either trans (control) or both trans and AdBACH1. Cells were harvested after a further 24-h incubation, and samples were prepared for either qPCR or WB assays ($n = 3$). (D) qPCR analysis of *HO-1* levels. n.s., not significant; ***, $P \leq 0.001$; **, $P \leq 0.01$. Significance was assessed with a one-way ANOVA. (E) WB showing exogenous BACH1 (FLAG) and endogenous HO-1 protein levels. GAPDH was used as a loading control.

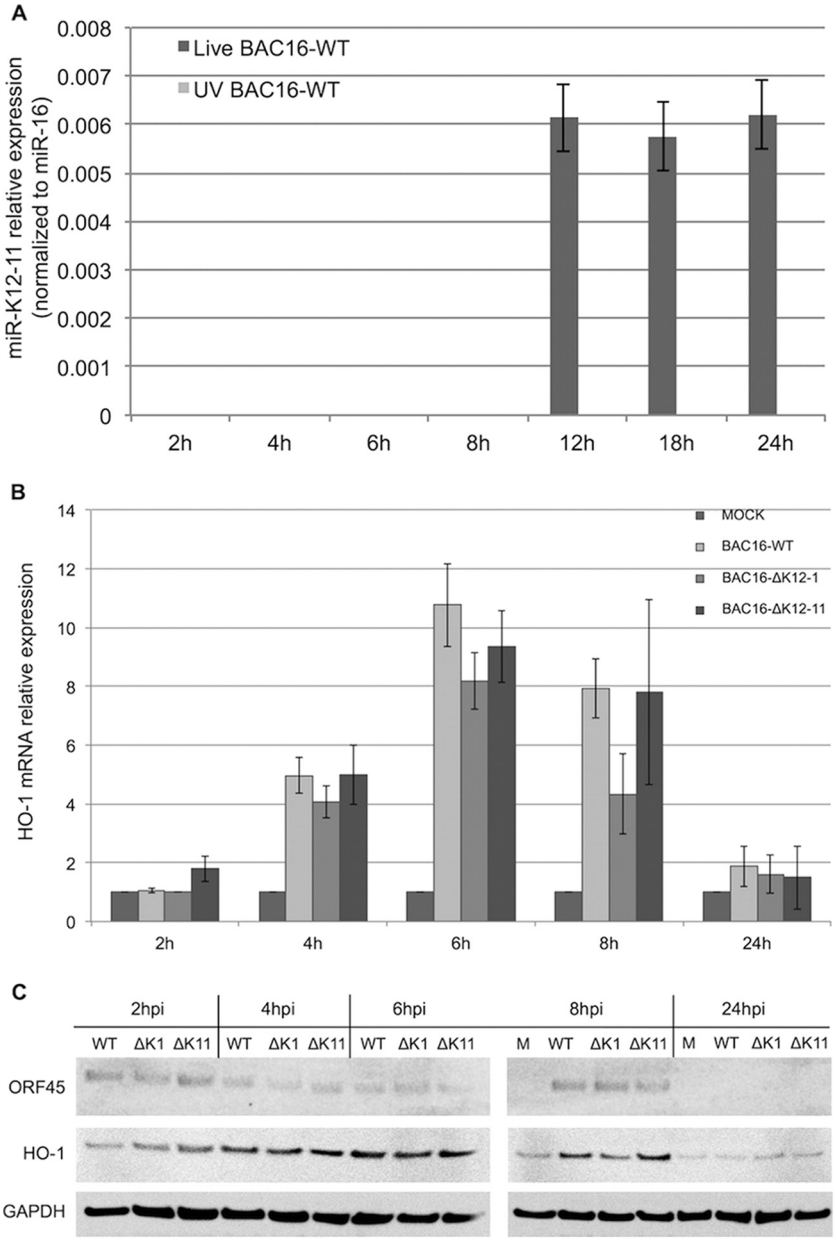

FIG 5 KSHV miR-K12-11 is not responsible for the early peak of HO-1 induction. (A to C) Time course experiments in which iLEC were infected with KSHV and then harvested at the indicated times thereafter. (A) Stem-loop qPCR assay of miR-K12-11 in cells infected with either live or UV-inactivated virus. miR-K12-11 expression is normalized to levels of the cellular internal control miR-16 ($n = 3$). (B) qPCR assay showing HO-1 mRNA levels ($n = 3$) in cells infected with WT or ΔK12-11 or ΔK12-1 mutant (as a control) KSHV. (C) WB showing HO-1 protein levels in mock-infected cells (M) or cells infected with the WT or ΔK12-11 (ΔK11) or ΔK12-1 (ΔK1) mutant (control) virus. The KSHV-encoded ORF45 protein was used as a marker of infection. GAPDH served as a loading control.

(100 μl) contained detectable levels of miR-K12-11, as well as other representative miRNAs and mRNAs (see Table S2 in the supplemental material). As expected, miR-K12-11 was not detected in the ΔK12-11 virus preparation, but we did observe measurable levels of other miRNAs and mRNAs therein. Using samples collected at multiple intervals over the first 24 hpi, we used a stem-loop qPCR assay to measure miRNA levels in iLEC infected with the live or UV-inactivated WT virus (Fig. 5A). Interestingly, despite the capacity of the UV-inactivated virus to induce early transient HO-1 (Fig. 1D and E), no miR-K12-11 was detected in cells infected with the UV-inactivated virus; cells infected with the live virus showed appreciable levels of the miRNA only by 12 hpi, presumably as a consequence of *de novo* transcription. Thus, considering the small inoculum volume used for KSHV infection (less than 1 μl of the stock preparation) and the inability to detect any miR-K12-11 prior to 12 hpi, our data suggest that miR-K12-11 is not responsible for the early HO-1 induction seen. In order to confirm this conclusion, iLEC were infected with the WT virus or the ΔK12-11 or ΔK12-1 mutant virus, and HO-1 levels were determined at early times postinfection (Fig. 5B and C). As expected, we were unable to detect miR-K12-11 in ΔK12-11 mutant-infected iLEC (see Fig. S5 in the supplemental material). HO-1

levels in ΔK12-11 mutant-infected iLEC were, however, comparable to those in cells infected with the WT and ΔK12-1 mutant viruses, confirming that this miRNA does not play a role in the early transient induction of HO-1 in KSHV-infected cells. Given the role of BACH1 in the negative regulation of HO-1 (Fig. 4), we also considered that BACH1 could influence early HO-1 expression independently of miR-K12-11 action. Thus, we examined the expression of BACH1 in KSHV-infected LEC over the first 8 h of infection (see Fig. S6). BACH1 expression was unaffected during that time, indicating that early induction of HO-1 is not as a consequence of BACH1 downregulation.

DISCUSSION

In the present study, we confirmed HO-1 upregulation in LEC infected with a BAC-derived KSHV. Under basal conditions, HO-1 expression is tightly regulated by the transcriptional repressor BACH1 (48). BACH1 mRNA is downregulated by KSHV through the action of the viral miRNA miR-K12-11, which targets the BACH1 3′ untranslated region (22, 23). It was recently shown that exogenous expression of miR-K12-11 in 293 cells is sufficient for both the induction of HO-1 and the concurrent downregulation of BACH1, suggesting an inverse correlation of the regulation of these two proteins (43). Our present study is the first to demonstrate that miR-K12-11 also targets BACH1 during *de novo* infection of LEC, with a concomitant increase in HO-1. Importantly, however, HO-1 levels in LEC infected with KSHV lacking miR-K12-11 (ΔK12-11) are not restored to those in mock-infected cells, indicating that the viral miRNA is not the sole element responsible for the modulation of this antioxidant pathway. It is not uncommon for viruses to adopt more than one mechanism to regulate key cellular proteins and pathways. Therefore, it is likely that other viral and/or cellular components modulate the expression of BACH1 and/or other HO-1 regulators, such as the transcriptional activator NRF2 (26, 49, 50). NRF2 (also known as NFE2L2) is a member of the basic region leucine zipper protein family and, as described above, plays a critical role in the induction of oxidative-stress-responsive genes such as *HO-1* (26, 51). Consequently, it is plausible that KSHV has developed the ability to modulate *HO-1* expression by regulating both BACH1 and NRF2. A recent report suggested that the KSHV latency protein vFLIP, by virtue of its ability to induce NRF2 during latent infection of human dermal microvascular EC (HMVEC-d) (52) could provide yet another means whereby KSHV modulates *HO-1* expression.

Another intriguing result is our finding that the subcellular localization of BACH1 is altered by KSHV infection of LEC, with a percentage of the predominantly nuclear protein being redistributed to the cytoplasm; as previously stated, BACH1 functions as a *HO-1* transcriptional repressor when bound to the *HO-1* promoter in the nucleus. Accordingly, KSHV could also impair BACH1-mediated repression of ARE-containing genes such as *HO-1* by preventing its translocation to the nucleus or inducing its nuclear export. Further investigation is needed to evaluate how KSHV mediates the relocalization of BACH1 and to identify the viral and/or host factors involved.

While investigating the kinetics of *HO-1* expression in *de novo*-infected LEC, we discovered that *HO-1* is also rapidly and transiently upregulated at early times postinfection (6 to 8 hpi). This early induction was not dependent on *de novo* expression of viral genes, since UV-inactivated virus induced similar levels of HO-1. This suggests that one or more virion components might be responsible for the transient upregulation seen. A recent paper demonstrated the presence of biologically functional viral miRNAs in KSHV virions (47). Thus, we investigated whether miR-K12-11 was also responsible for the early induction of HO-1. Despite the detection of miR-K12-11 in stock virus preparations, our data indicate that this viral miRNA is not responsible for the early induction of HO-1. Consequently, we predict that another virion component(s) is responsible for the early induction of HO-1. Since cellular pathways regulated by early *de novo* KSHV infection are thought to participate in the orchestration of effective viral infection (53), it is reasonable to speculate that early induction of HO-1 by KSHV could protect the cell from virus-induced oxidative stress and contribute to a cellular environment permissive for successful infection. The recent finding that NRF2 induction in KSHV-infected HMVEC-d is regulated by early *de novo* infection events, including virus binding and early signaling (52), suggests that KSHV induction of NRF2 contributes to the early HO-1 peak seen in KSHV-infected LEC. The long-term goal of our studies is to develop a novel therapy for KS. Because of the selective pressure on the virus that can lead to mutations within its genome, drug resistance is a recurrent problem when targeting viral genes (54, 55). Therefore, a more attractive strategy involves the identification of cellular genes that are uniquely expressed or overexpressed during the development of the pathology. HO-1 may represent such a target for the treatment of KS: HO-1 is selectively upregulated in KS spindle cells (7), KS lesions are characterized by high free heme and hemoglobin levels as a result of erythrocyte extravasation and degradation (56–58), and HO-1 induction affords survival and proliferation advantages to infected cells within the unique tumor microenvironment that would otherwise be hostile to normal cells. For these reasons and because HO-1 targeting has been successful in the treatment of other types of cancer, we propose that a similar approach should be considered for the treatment of KS.

MATERIALS AND METHODS

Cells and viruses. Primary adult human LEC were obtained from Lonza (Allendale, NJ). iLEC were generated from these cells via transduction with a retrovirus expressing papillomavirus E6/E7 as previously described (41). LEC were cultured in EGM-2 medium prepared by supplementing basal medium (EBM-2; Lonza) with 10% fetal bovine serum (FBS), penicillin-streptomycin–L-glutamine (PSG; HyClone, Logan, UT), and additional EC growth supplements (EGM-2MV Bullet kit; Lonza). HEK293T cells were grown in Dulbecco's modified Eagle's medium (DMEM) supplemented with 10% FBS and PSG. Epithelial iSLK cells (generously provided by Rolf Renne at the University of Florida, Gainesville, FL, with kind permission from Jae Jung at the University of Southern California, Los Angeles, CA, and Don Ganem at the University of California, San Francisco, CA) were used to produce stocks of recombinant KSHV (35, 44, 59, 60). iSLK cells were grown in DMEM supplemented with 10% FBS, PSG, puromycin (1 μg/ml), neomycin (200 μg/ml), and hygromycin (1.5 mg/ml). The KSHV BAC clone BAC16 was kindly provided by Jae Jung (35). KSHV-BAC16 was derived from recombinant rKSHV.219, which expresses GFP under the control of the human EF1α promoter (61). The independent regulation of GFP and viral gene expression in this virus leads to occasional cells that express discordant levels of KSHV and LANA (62, 63). To produce stocks of recombinant KSHV, iSLK cells harboring BAC16 were treated with doxycycline (1 μM) and sodium butyrate (3 mM) for 72 h. Supernatants were then collected, and cell debris was removed via low-speed centrifugation. Clarified supernatants were then transferred to ultracentrifuge tubes, underlaid with 25% sucrose in TNE (150 mM NaCl, 10 mM Tris [pH 8.0], 2 mM EDTA

[pH 8.0]), and centrifuged at 78,000 × *g* for 2 h at 4°C. The resulting virion pellets were resuspended in TNE. Stocks of BAC16-derived KSHV were titrated by infecting iLEC with serially diluted virus preparations. After a 48-h incubation, the cells were harvested and evaluated for GFP expression via flow cytometry. For latent-infection experiments, the MOI (multiplicity of infection) was normalized to the volume of viral supernatant required for 20% GFP^+ iLEC. For acute-infection experiments, MOIs corresponding to 80% GFP^+ iLEC were used and centrifugation was omitted in order to prevent mechanical-stress-induced *HO-1* upregulation.

Antibodies and other reagents. HO-1 protein levels were assessed with a mouse anti-HO-1 monoclonal antibody (MAb; BD Transduction Laboratories, Franklin Lakes, NJ) at concentrations of 1:1,000 for Western blotting (WB) and 1:200 for IFA and flow cytometry. An anti-GFP (goat) horseradish peroxidase (HRP)-conjugated antibody (600-103-215; Rockland, Limerick, PA) was used at 1:2,000 in order to detect GFP. Mouse anti-BACH1 (F-9) antibody (sc-271211; Santa Cruz Biotechnologies, Santa Cruz, CA) was used at either 1:200 (WB) or 1:100 (IFA). Glyceraldehyde 3-phosphate dehydrogenase (GAPDH) levels were used as WB loading controls and detected with a mouse anti-GAPDH antibody (ab8245; Abcam, Cambridge, England) at a concentration of 1:20,000. Mouse anti-ORF45 antibody (ab36618; Abcam) was used at 1:500 (WB). A rabbit anti-LANA antibody (UK183), kindly provided by Bala Chandran (Rosalind Franklin University, Chicago, IL) was used at 1:100 for IFA. For FLAG epitope detection, an anti-FLAG M2 HRP-conjugated MAb (Sigma, St. Louis, MO) was used at 1:5,000. For WB, donkey anti-rabbit (sc-2313; Santa Cruz Biotechnologies) or HRP-conjugated goat anti-mouse (Millipore, Billerica, MA) secondary antibodies were each used at a concentration of 1:10,000. For IFA, Alexa Fluor 594-conjugated anti-mouse IgG1 and Alexa Fluor 647-conjugated anti-rabbit secondary antibodies (both from Invitrogen, Eugene, OR) were used at 1:1,000. miRNA mimics were transfected into iLEC with Effectene (Qiagen, Valencia, CA). Both the miR-K12-11 mimic (KSHV-miR-K12-11-5p *mir*Vana miRNA mimic) and the negative-control miRNA (6-carboxyfluorescein dye-labeled control pre-miR) were purchased from Ambion (Life Technologies, Carlsbad, CA).

BACH1 adenovirus vector. A FLAG tag was fused to the BACH1 N terminus by standard PCR techniques. The resulting DNA fragment was cloned into the adenoviral vector pAdTet7. In this vector, transgene expression is driven by a minimal cytomegalovirus promoter that is preceded by multiple Tet repressor binding sites. Expression from this chimeric promoter takes place only in the presence of the Tet transactivator, as well as the absence of tetracycline or doxycycline (a so-called "Tet-off" system). In this system, the Tet transactivator is expressed from a second coinfecting adenovirus, here referred to as trans. In all AdBACH1 experiments, cells infected with trans alone were used to control for nonspecific effects resulting from adenoviral infection (64). Adenovirus was prepared from these vectors as described previously (46).

Reverse transcription-qPCR assay. Extraction of total RNA was performed with miRNeasy minikits (Qiagen, Valencia, CA), which allow the isolation of both miRNAs and mRNAs. DNase I (Qiagen) digestion was included to remove any contaminating DNA from the samples. Total cDNA was generated from these samples with the SuperScript III First-Strand Synthesis System (Invitrogen; Life Technologies, Carlsbad, CA). The following stem-loop PCR primers were used for the reverse transcription of miRNAs (stem-loop [SL] reverse transcription) as previously described (65): mir-k12-11 SL, 5′-GTCGTATCCAGTGCAGGGTCCGAGGTATTCGCACTGGATACGACTCGGAC-3′; mir-k12-1 SL, 5′-GTCGTATCCAGTGCAGGGTCCGAGGTATTCGCACTGGATACGACGCTTAC-3′; mir16 SL, 5′-GTCGTATCCAGTGCAGGGTCCGAGGTATTCGCACTGGATACGACCGCCAA-3′; mir-155 SL, 5′-GTCGTATCCAGTGCAGGGTCCGAGGTATTCGCACTGGATACGACACCCCT-3′. The following primers were used for qPCR assays of mRNAs: GAPDH F, 5′-GAAGGTGAAGGTCGGAGT-3′; GAPDH R, 5′-GAAGATGGTGATGGGATTTC-3′; HO-1 F, 5′-GCCCTTCAGCATCCTCAGTTC-3′; HO-1 R, 5′-GGTTTGAGACAGCTGCCACA-3′; BACH1 F, 5′-TGAGAAGCTGCAAAGTGAAAAGG-3′; BACH1 R, 5′-CTGCTTTGTCTCACCCAGAGT-3′; ORF59 F 5′-CGAGTCTTCGCAAAAGGTTC-3′; ORF59 R, 5′-AAGGGACCAACTGGTGTGAG-3′. The following primers were used for qPCR assays of miRNAs: miR-K12-11 F, 5′-CGAGCCTTAATGCTTAGCCUG-3′; miR-K12-1 F, 5′-GCGAGCATTACAGGAAACTGG-3′; miR16 F, 5′-CGGCAGTAGCAGCACGTAAAT-3′; miR-155 F, 5′-CGCGAGCTTAATGCTAATCGTG-3′. The reverse primer used for miRNA detection was Universal SL Rev (5′-CCAGTGCAGGGTCCGAGGTA-3′). To perform a qPCR assay, 5 μl of cDNA (typically, 1 to 10 ng) was mixed with gene-specific primers and 12.5 μl of Power SYBR green PCR master mix (ABI, Foster City, CA) to a final volume of 25 μl. Optimization of primer and sample concentrations was performed for all targets. For qPCR assay experiments, standard curves were set up with appropriate control samples and a dilution series ranging from 100 ng to 3.2 pg of cDNA. Sample amplification was performed with an ABI real-time PCR 7500 system. For relative quantitation experiments, the signal for each cDNA was normalized to GAPDH levels, thereby allowing the comparison of mRNA expression levels in different samples.

WB analysis. Cells were lysed in radioimmunoprecipitation assay buffer (50 mm Tris [pH 7.5], 150 mm NaCl, 1% Nonidet P-40, 0.5% deoxycholate, 0.1% SDS, 1× Complete inhibitors [Roche Applied Science, Pleasanton, CA]), incubated on ice for 30 min, and then centrifuged at 13,400 × *g* for 10 min at 4°C. Cleared supernatants were transferred to fresh tubes, and their protein concentrations were determined via bicinchoninic acid assay (Thermo Fisher Scientific, Waltham, MA). The resulting proteins were separated via reducing SDS-PAGE, transferred to polyvinylidene difluoride membranes, incubated in blocking buffer (5% nonfat dry milk in Tris-buffered saline with 0.1% Tween 20 [TBST]) for 1 h with agitation, and then probed with the appropriate primary antibody diluted in blocking buffer. Blots were then washed three times with TBST, incubated with the appropriate secondary antibodies in blocking buffer, and then washed a further three times with TBST. Blots were developed with an ECL Plus kit (Amersham Biosciences/GE Healthcare, Pittsburgh, PA), and the resulting data were captured with either Kodak XAR film or a G:BOX (Syngene). The ImageJ software package (ImageJ; National Institutes of Health, Bethesda, MD; http://imagej.nih.gov/ij/) was used for band quantitation. The images shown are representative of three independent experiments.

IFA and image analysis. For IFA, cells were seeded onto collagen-coated coverslips (BD Biosystems, Franklin Lakes, NJ) in six-well tissue culture plates. At the end of the experiment, cells were fixed in 2% paraformaldehyde for 8 min, washed three times in phosphate-buffered saline (PBS), and permeabilized in 0.25% Triton X-100 for 8 min. Cells were blocked in IFA blocking buffer (20% normal goat serum [NGS] in PBS) for 20 min at 37°C and incubated with the appropriate primary antibody incubation buffer (1% NGS in PBS) for 1 h at 37°C. After primary antibody incubation, coverslips were washed three times in PBS and incubated with both the appropriate secondary antibody and the nuclear stain 4′,6-diamidino-2-phenylindole (DAPI) for 45 min at 37°C. Coverslips were then washed three times in PBS and mounted on glass slides with Fluoromount-G (Southern Biotech, Birmingham, AL). The slides were then analyzed with a DeltaVision real-time deconvolution fluorescence microscope (Applied Precision, Issaquah, WA), and images were captured with a Photometrics CoolSNAP HQ camera. Image analysis was performed with SoftWoRx (Applied Precision). Stacks of images (0.2-μm z step) were captured at ×60 magnification. Stacks were subjected to deconvolution, and two- or three-section projections were made by superimposing representative z planes to generate the final image. Images shown are representative of three independent experiments. Where necessary to facilitate visualization of GFP and more than one fluorescently tagged target protein of interest, GFP was pseudocolored to grayscale.

Flow cytometry. Cells to be analyzed via flow cytometry were dissociated from tissue culture plates with nonenzymatic Cellstripper (25-056-CI; Cellgro/Corning, Manassas, VA) and then pelleted at 1,800 × *g* at 4°C for 5 min.

The cells were fixed with BD Cytofix/Cytoperm, incubated on ice for 15 min, pelleted, and then resuspended in 1× BD Permwash containing the primary antibody. After a further 15-min incubation on ice, the cells were washed three times and then resuspended in 1× BD Permwash containing the appropriate dilution of the secondary antibody. After a subsequent 15 min on ice, the cells were washed in 1× BD Permwash and finally analyzed on a BD FACSCalibur flow cytometer (BD Biosciences).

Statistical analysis. Quantitative PCR data are expressed as the mean ± the standard error of the mean (SEM). Statistical analysis was performed with R software (R Core Team, Vienna, Austria). One-way analysis of variance (ANOVA) and Kruskal-Wallis tests were used to compare means of different groups.

SUPPLEMENTAL MATERIAL

Supplemental material for this article may be found at http://mbio.asm.org/lookup/suppl/doi:10.1128/mBio.00668-15/-/DCSupplemental.

Figure S1, TIF file, 2.1 MB.
Figure S2, TIF file, 2.7 MB.
Figure S3, TIF file, 1.7 MB.
Figure S4, TIF file, 1.3 MB.
Figure S5, TIF file, 1.4 MB.
Figure S6, TIF file, 1.2 MB.
Table S1, PDF file, 0.04 MB.
Table S2, PDF file, 0.04 MB.

ACKNOWLEDGMENTS

This research was supported by grants R01 CA099906 (A.V.M.), ONPRC P51 OD011092 (A.V.M., J.K.G.), and T32 AI007472 (J.E.T.) from the NIH and award 14PRE20320014 from the America Heart Association (S.B.).

We thank Lisa Clepper and Jessica Osborn for technical assistance, Djamil Legato for assistance with manuscript and figure preparation, and Byung S. Park for his support with statistical analysis.

REFERENCES

1. **Wen KW, Damania B.** 2010. Kaposi sarcoma-associated herpesvirus (KSHV): molecular biology and oncogenesis. Cancer Lett **289:**140–150. http://dx.doi.org/10.1016/j.canlet.2009.07.004.
2. **Mesri EA, Cesarman E, Boshoff C.** 2010. Kaposi's sarcoma and its associated herpesvirus. Nat Rev Cancer **10:**707–719. http://dx.doi.org/10.1038/nrc2888.
3. **Martin D, Gutkind JS.** 2008. Human tumor-associated viruses and new insights into the molecular mechanisms of cancer. Oncogene **27**(Suppl 2): S31–S42. http://dx.doi.org/10.1038/onc.2009.351.
4. **Ganem D.** 2012. KSHV infection and the pathogenesis of Kaposi's sarcoma. Annu Rev Pathol Mech Dis **1:**1–26. http://dx.doi.org/10.1146/annurev.pathol.1.110304.100133.
5. **Giffin L, Damania B.** 2014. KSHV: pathways to tumorigenesis and persistent infection. Adv Virus Res **88:**111–159. http://dx.doi.org/10.1016/B978-0-12-800098-4.00002-7.
6. **Lee H-R, Brulois K, Wong L, Jung JU.** 2012. Modulation of immune system by Kaposi's sarcoma-associated herpesvirus: lessons from viral evasion strategies. Front Microbiol **3:**44. http://dx.doi.org/10.3389/fmicb.2012.00044.
7. **McAllister SC, Hansen SG, Ruhl RA, Raggo CM, DeFilippis VR, Greenspan D, Früh K, Moses AV.** 2004. Kaposi sarcoma-associated herpesvirus (KSHV) induces heme oxygenase-1 expression and activity in KSHV-infected endothelial cells. Blood **103:**3465–3473. http://dx.doi.org/10.1182/blood-2003-08-2781.
8. **Raggo C, Ruhl R, McAllister S, Koon H, Dezube BJ, Früh K, Moses AV.** 2005. Novel cellular genes essential for transformation of endothelial cells by Kaposi's sarcoma-associated herpesvirus. Cancer Res **65:**5084–5095. http://dx.doi.org/10.1158/0008-5472.CAN-04-2822.
9. **Abraham NG, Kappas A.** 2008. Pharmacological and clinical aspects of heme oxygenase. Pharmacol Rev **60:**79–127. http://dx.doi.org/10.1124/pr.107.07104.
10. **Banerjee P, Basu A, Wegiel B, Otterbein LE, Mizumura K, Gasser M, Waaga-Gasser AM, Choi AM, Pal S.** 2012. Heme oxygenase-1 promotes survival of renal cancer cells through modulation of apoptosis- and autophagy-regulating molecules. J Biol Chem **287:**32113–32123. http://dx.doi.org/10.1074/jbc.M112.393140.
11. **Gozzelino R, Jeney V, Soares MP.** 2010. Mechanisms of cell protection by heme oxygenase-1. Annu Rev Pharmacol Toxicol **50:**323–354. http://dx.doi.org/10.1146/annurev.pharmtox.010909.105600.
12. **Miyazaki T, Kirino Y, Takeno M, Samukawa S, Hama M, Tanaka M, Yamaji S, Ueda A, Tomita N, Fujita H, Ishigatsubo Y.** 2010. Expression of heme oxygenase-1 in human leukemic cells and its regulation by transcriptional repressor Bach 1. Cancer Sci **101:**1409–1416. http://dx.doi.org/10.1111/j.1349-7006.2010.01550.x.
13. **Do MT, Kim HG, Khanal T, Choi JH, Kim DH, Jeong TC, Jeong HG.** 2013. Metformin inhibits heme oxygenase-1 expression in cancer cells through inactivation of Raf-ERK-Nrf2 signaling and AMPK-independent pathways. Toxicol Appl Pharmacol **271:**229–238. http://dx.doi.org/10.1016/j.taap.2013.05.010.
14. **Berberat PO, Dambrauskas Z, Gulbinas A, Giese T, Giese N, Künzli B, Autschbach F, Meuer S, Büchler MW, Friess H.** 2005. Inhibition of heme oxygenase-1 increases responsiveness of pancreatic cancer cells to anticancer treatment. Clin Cancer Res **11:**3790–3798. http://dx.doi.org/10.1158/1078-0432.CCR-04-2159.
15. **Lin P-H, Lan W-M, Chau L-Y.** 2013. TRC8 suppresses tumorigenesis through targeting heme oxygenase-1 for ubiquitination and degradation. Oncogene **32:**2325–2334. http://dx.doi.org/10.1038/onc.2012.244.
16. **Ryter SW, Alam J, Choi AM.** 2006. Heme oxygenase-1/carbon monoxide: from basic science to therapeutic applications. Physiol Rev **86:**583–650. http://dx.doi.org/10.1152/physrev.00011.2005.
17. **Paine A, Eiz-Vesper B, Blasczyk R, Immenschuh S.** 2010. Signaling to heme oxygenase-1 and its anti-inflammatory therapeutic potential. Biochem Pharmacol **80:**1895–1903. http://dx.doi.org/10.1016/j.bcp.2010.07.014.
18. **Ferrándiz ML, Devesa I.** 2008. Inducers of heme oxygenase-1. Curr Pharm Des **14:**473–486. http://dx.doi.org/10.2174/138161208783597399.
19. **Bartel DP.** 2004. MicroRNAs: genomics, biogenesis, mechanism, and function. Cell **116:**281–297. http://dx.doi.org/10.1016/S0092-8674(04)00045-5.
20. **Grey F, Hook L, Nelson J.** 2008. The functions of herpesvirus-encoded microRNAs. Med Microbiol Immunol **197:**261–267. http://dx.doi.org/10.1007/s00430-007-0070-1.
21. **Gottwein E.** 2012 Kaposi's sarcoma-associated herpesvirus microRNAs. Front Microbiol **3:**165. http://dx.doi.org/10.3389/fmicb.2012.00165.
22. **Gottwein E, Mukherjee N, Sachse C, Frenzel C, Majoros WH, Chi JT, Braich R, Manoharan M, Soutschek J, Ohler U, Cullen BR.** 2007. A viral microRNA functions as an orthologue of cellular miR-155. Nature **450:**1096–1099. http://dx.doi.org/10.1038/nature05992.
23. **Skalsky RL, Samols MA, Plaisance KB, Boss IW, Riva A, Lopez MC, Baker HV, Renne R.** 2007. Kaposi's sarcoma-associated herpesvirus encodes an ortholog of miR-155. J Virol **81:**12836–12845. http://dx.doi.org/10.1128/JVI.01804-07.
24. **Sun J, Hoshino H, Takaku K, Nakajima O, Muto A, Suzuki H, Tashiro S, Takahashi S, Shibahara S, Alam J, Taketo MM, Yamamoto M, Igarashi K.** 2002. Hemoprotein Bach1 regulates enhancer availability of heme oxygenase-1 gene. EMBO J **21:**5216–5224. http://dx.doi.org/10.1093/emboj/cdf516.
25. **Malhotra D, Portales-Casamar E, Singh A, Srivastava S, Arenillas D, Happel C, Shyr C, Wakabayashi N, Kensler TW, Wasserman WW, Biswal S.** 2010. Global mapping of binding sites for Nrf2 identifies novel targets in cell survival response through ChIP-Seq profiling and network analysis. Nucleic Acids Res **38:**5718–5734. http://dx.doi.org/10.1093/nar/gkq212.
26. **Shan Y, Lambrecht RW, Donohue SE, Bonkovsky HL.** 2006. Role of Bach1 and Nrf2 in up-regulation of the heme oxygenase-1 gene by cobalt protoporphyrin. FASEB J **20:**2651–2653. http://dx.doi.org/10.1096/fj.06-6346fje.
27. **Warnatz H-J, Schmidt D, Manke T, Piccini I, Sultan M, Borodina T, Balzereit D, Wruck W, Soldatov A, Vingron M, Lehrach H, Yaspo ML.** 2011. The BTB and CNC homology 1 (BACH1) target genes are involved in the oxidative stress response and in control of the cell cycle. J Biol Chem **286:**23521–23532. http://dx.doi.org/10.1074/jbc.M111.220178.
28. **Ogawa H, Ishiguro K, Gaubatz S, Livingston DM, Nakatani Y.** 2002. A complex with chromatin modifiers that occupies E2F- and Myc-responsive genes in G_0 cells. Science **296:**1132–1136. http://dx.doi.org/10.1126/science.1069861.
29. **Sun J, Brand M, Zenke Y, Groudine M, Igarashi K.** 2004. Heme regulates

the dynamic exchange of Bach1 and NF-E2-related factors in the Maf transcription factor network. Proc Natl Acad Sci U S A **101:**1461–1466. http://dx.doi.org/10.1073/pnas.0308083100.
30. **Elton TS, Selemon H, Elton SM, Parinandi NL.** 2013. Regulation of the MIR155 host gene in physiological and pathological processes. Gene **532:** 1–12. http://dx.doi.org/10.1016/j.gene.2012.12.009.
31. **Boss IW, Nadeau PE, Abbott JR, Yang Y, Mergia A, Renne R.** 2011. A Kaposi's sarcoma-associated herpesvirus-encoded ortholog of microRNA miR-155 induces human splenic B-cell expansion in NOD/LtSz-scid IL2Rγnull mice. J Virol **85:**9877–9886. http://dx.doi.org/10.1128/JVI.05558-11.
32. **Sin S-H, Kim YB, Dittmer DP.** 2013. Latency locus complements microRNA 155 deficiency *in vivo*. J Virol **87:**11908–11911. http://dx.doi.org/10.1128/JVI.01620-13.
33. **Abend JR, Ramalingam D, Kieffer-Kwon P, Uldrick TS, Yarchoan R, Ziegelbauer JM.** 2012. Kaposi's sarcoma-associated herpesvirus microRNAs target IRAK1 and MYD88, two components of the Toll-like receptor/interleukin-1R signaling cascade, to reduce inflammatory-cytokine expression. J Virol **86:**11663–11674. http://dx.doi.org/10.1128/JVI.01147-12.
34. **Qin Z, Freitas E, Sullivan R, Mohan S, Bacelieri R, Branch D, Romano M, Kearney P, Oates J, Plaisance K, Renne R, Kaleeba J, Parsons C.** 2010. Upregulation of xCT by KSHV-encoded microRNAs facilitates KSHV dissemination and persistence in an environment of oxidative stress. PLoS Pathog **6:**e1000742. http://dx.doi.org/10.1371/journal.ppat.1000742.s004.
35. **Brulois KF, Chang H, Lee AS, Ensser A, Wong LY, Toth Z, Lee SH, Lee HR, Myoung J, Ganem D, Oh TK, Kim JF, Gao SJ, Jung JU.** 2012. Construction and manipulation of a new Kaposi's sarcoma-associated herpesvirus bacterial artificial chromosome clone. J Virol **86:**9708–9720. http://dx.doi.org/10.1128/JVI.01019-12.
36. **Cancian L, Hansen A, Boshoff C.** 2013. Cellular origin of Kaposi's sarcoma and Kaposi's sarcoma-associated herpesvirus-induced cell reprogramming. Trends Cell Biol **23:**421–432. http://dx.doi.org/10.1016/j.tcb.2013.04.001.
37. **Chang H, Ganem D.** 2013. A unique herpesviral transcriptional program in KSHV-infected lymphatic endothelial cells leads to mTORC1 activation and rapamycin sensitivity. Cell Host Microbe **13:**429–440. http://dx.doi.org/10.1016/j.chom.2013.03.009.
38. **Hong Y-K, Foreman K, Shin JW, Hirakawa S, Curry CL, Sage DR, Libermann T, Dezube BJ, Fingeroth JD, Detmar M.** 2004. Lymphatic reprogramming of blood vascular endothelium by Kaposi sarcoma-associated herpesvirus. Nat Genet **36:**683–685. http://dx.doi.org/10.1038/ng1383.
39. **Wang H-W, Trotter MW, Lagos D, Bourboulia D, Henderson S, Mäkinen T, Elliman S, Flanagan AM, Alitalo K, Boshoff C.** 2004. Kaposi sarcoma herpesvirus-induced cellular reprogramming contributes to the lymphatic endothelial gene expression in Kaposi sarcoma. Nat Genet **36:** 687–693. http://dx.doi.org/10.1038/ng1384.
40. **Carroll PA, Brazeau E, Lagunoff M.** 2004. Kaposi's sarcoma-associated herpesvirus infection of blood endothelial cells induces lymphatic differentiation. Virology **328:**7–18. http://dx.doi.org/10.1016/j.virol.2004.07.008.
41. **Moses AV, Fish KN, Ruhl R, Smith PP, Strussenberg JG, Zhu L, Chandran B, Nelson JA.** 1999. Long-term infection and transformation of dermal microvascular endothelial cells by human herpesvirus 8. J Virol **73:**6892–6902.
42. **Gottlieb Y, Truman M, Cohen LA, Leichtmann-Bardoogo Y, Meyron-Holtz EG.** 2012. Endoplasmic reticulum anchored heme-oxygenase-1 faces the cytosol. Haematologica **97:**1489–1493. http://dx.doi.org/10.3324/haematol.2012.063651.
43. **Gallaher AM, Das S, Xiao Z, Andresson T, Kieffer-Kwon P, Happel C, Ziegelbauer J.** 2013. Proteomic screening of human targets of viral microRNAs reveals functions associated with immune evasion and angiogenesis. PLoS Pathog **9:**e1003584. http://dx.doi.org/10.1371/journal.ppat.1003584.
44. **Plaisance-Bonstaff K, Choi HS, Beals T, Krueger BJ, Boss IW, Gay LA, Haecker I, Hu J, Renne R.** 2014. KSHV miRNAs decrease expression of lytic genes in latently infected PEL and endothelial cells by targeting host transcription factors. Viruses **6:**4005–4023. http://dx.doi.org/10.3390/v6104005.
45. **Skalsky RL, Cullen BR.** 2010. Viruses, microRNAs, and host interactions. Annu Rev Microbiol **64:**123–141. http://dx.doi.org/10.1146/annurev.micro.112408.134243.
46. **Hardy S, Kitamura M, Harris-Stansil T, Dai Y, Phipps ML.** 1997. Construction of adenovirus vectors through Cre-lox recombination. J Virol **71:**1842–1849.
47. **Lin X, Li X, Liang D, Lan K.** 2012. MicroRNAs and unusual small RNAs discovered in Kaposi's sarcoma-associated herpesvirus virions. J Virol **86:** 12717–12730. http://dx.doi.org/10.1128/JVI.01473-12.
48. **Dhakshinamoorthy S, Jain AK, Bloom DA, Jaiswal AK.** 2005. Bach1 competes with Nrf2 leading to negative regulation of the antioxidant response element (ARE)-mediated NAD(P)H:quinone oxidoreductase 1 gene expression and induction in response to antioxidants*. J Biol Chem **280:**16891–16900. http://dx.doi.org/10.1074/jbc.M500166200.
49. **Lee Y-M, Auh Q-S, Lee D-W, Kim JY, Jung HJ, Lee SH, Kim EC.** 2013. Involvement of Nrf2-mediated upregulation of heme oxygenase-1 in mollugin-induced growth inhibition and apoptosis in human oral cancer cells. Biomed Res Int **2013:**210604. http://dx.doi.org/10.1155/2013/210604.
50. **Inamdar NM, Ahn YI, Alam J.** 1996. The heme-responsive element of the mouse heme oxygenase-1 gene is an extended AP-1 binding site that resembles the recognition sequences for MAF and NF-E2 transcription factors. Biochem Biophys Res Commun **221:**570–576. http://dx.doi.org/10.1006/bbrc.1996.0637.
51. **Zhang J, Ohta T, Maruyama A, Hosoya T, Nishikawa K, Maher JM, Shibahara S, Itoh K, Yamamoto M.** 2006. BRG1 interacts with Nrf2 to selectively mediate HO-1 induction in response to oxidative stress. Mol Cell Biol **26:**7942–7952. http://dx.doi.org/10.1128/MCB.00700-06.
52. **Gjyshi O, Bottero V, Veettil MV, Dutta S, Singh VV, Chikoti L, Chandran B.** 2014. Kaposi's sarcoma-associated herpesvirus induces Nrf2 during *de novo* infection of endothelial cells to create a microenvironment conducive to infection. PLoS Pathog **10:**e1004460. http://dx.doi.org/10.1371/journal.ppat.1004460.
53. **Chandran B.** 2010. Early events in Kaposi's sarcoma-associated herpesvirus infection of target cells. J Virol **84:**2188–2199. http://dx.doi.org/10.1128/JVI.01334-09.
54. **Coen N, Duraffour S, Topalis D, Snoeck R, Andrei G.** 2014. Spectrum of activity and mechanisms of resistance of various nucleoside derivatives against γ-herpesviruses. Antimicrob Agents Chemother **58:**7312–7323. http://dx.doi.org/10.1128/AAC.03957-14.
55. **Dittmer DP, Krown SE.** 2007. Targeted therapy for Kaposi's sarcoma and Kaposi's sarcoma-associated herpesvirus. Curr Opin Oncol **19:**452–457. http://dx.doi.org/10.1097/CCO.0b013e3281eb8ea7.
56. **Wang L, Damania B.** 2008. Kaposi's sarcoma-associated herpesvirus confers a survival advantage to endothelial cells. Cancer Res **68:**4640–4648. http://dx.doi.org/10.1158/0008-5472.CAN-07-5988.
57. **Dittmer DP, Damania B.** 2013. Kaposi sarcoma associated herpesvirus pathogenesis (KSHV)—an update. Curr Opin Virol **3:**238–244. http://dx.doi.org/10.1016/j.coviro.2013.05.012.
58. **Orenstein JM.** 2008. Ultrastructure of Kaposi sarcoma. Ultrastruct Pathol **32:**211–220. http://dx.doi.org/10.1080/01913120802343871.
59. **Myoung J, Ganem D.** 2011. Generation of a doxycycline-inducible KSHV producer cell line of endothelial origin: maintenance of tight latency with efficient reactivation upon induction. J Virol Methods **174:**12–21. http://dx.doi.org/10.1016/j.jviromet.2011.03.012.
60. **Stürzl M, Gaus D, Dirks WG, Ganem D, Jochmann R.** 2013. Kaposi's sarcoma-derived cell line SLK is not of endothelial origin, but is a contaminant from a known renal carcinoma cell line. Int J Cancer **132:** 1954–1958. http://dx.doi.org/10.1002/ijc.27849.
61. **Vieira J, O'Hearn PM.** 2004. Use of the red fluorescent protein as a marker of Kaposi's sarcoma-associated herpesvirus lytic gene expression. Virology **325:**225–240. http://dx.doi.org/10.1016/j.virol.2004.03.049.
62. **Ellison TJ, Kedes DH.** 2014. Variable episomal silencing of a recombinant herpesvirus renders its encoded GFP an unreliable marker of infection in primary cells. PLoS One **9:**e111502. http://dx.doi.org/10.1371/journal.pone.0111502.t002.
63. **Jeffery HC, Wheat RL, Blackbourn DJ, Nash GB, Butler LM, Jeffery HC, Wheat RL, Blackbourn DJ, Nash GB, Butler LM.** 2013. Infection and transmission dynamics of rKSHV.219 in primary endothelial cells. J Virol Methods **193:**251–259. http://dx.doi.org/10.1016/j.jviromet.2013.06.001.
64. **Altschuler Y, Barbas SM, Terlecky LJ, Tang K, Hardy S, Mostov KE, Schmid SL.** 1998. Redundant and distinct functions for dynamin-1 and dynamin-2 isoforms. J Cell Biol **143:**1871–1881. http://dx.doi.org/10.1083/jcb.143.7.1871.
65. **Kramer MF, Coen DM.** 2001. Enzymatic amplification of DNA by PCR: standard procedures and optimization. Curr Protoc Mol Biol Chapter **15:**Unit 15.1. http://dx.doi.org/10.1002/0471142727.mb1510s95.